Backscattering value estimation with Rayleigh approximation

August 31, 2020

Contents

1 Introduction

This report is mainly about using radiative transfer method to model scattering of electromagnetic radiation by vegetation canopies. During the modelling, we will treat the vegetation canopies as Rayleigh particles. The whole procedure is based on the Single-Scattering Radiative Transfer Model provided in [1]. Two areas over Hengshui area, North China Plain are used to test the model. Sentinel-2 generated LAI and C_w are used to compute the extinction and scattering coefficient of canopy. Time series in-situ soil moisture are used to compute the permittivity of soils.

2 Extinction and scattering coefficient of canopy

2.1 Gravimetric water content computation

Models describing the scattering and emission behavior of a vegetation canopy are often developed in terms of the volume absorption and scattering coefficients of the canopy. In general, both quantities are governed by the

permittivity, volume fraction, and geometry (i.e., the shape and orientation relative to the EM wave's electric field) of the various types of inclusions present in the canopy. Gravimetric water content is one main factor that affects the permittivity of canopy changes. In this section, we introduce the computation of canopy gravimetric water content.

Leaf equivalent water thickness $C_{w,l}(g/cm^2)$ is calculated as [2]

$$C_{wl} = \frac{M_{lw} - M_{ld}}{A} \tag{1}$$

where M_{lw} is the fresh mass of leaf samples, M_{ld} is the dry mass. Then, the canopy water content $C_w(kg/m^2)$ is calculated as

$$\begin{aligned} C_w &= C_{wl} \times \mathrm{LAI}(g/cm^2) \\ &= 10 \times C_{wl} \times \mathrm{LAI}(kg/m^2) \end{aligned} \tag{2}$$

The volumetric water content is given as

$$m_v = C_w \times l \times \rho_w \tag{3}$$

where l (m), the leaf thickness and ρ_w is the water density ($997kg/m^3$). According to [3], the wheat thickness is $0.2mm$.

Then, the gravimetric water content is computed as [4]

$$m_g = \frac{m_w - m_d}{m_w} \tag{4}$$

where m_w and m_d are the wet weight of the vegetation sample, and its dry weight. The gravimetric water content and volumetric water content m_v (kg/m^3) are related by [1]

$$m_g = \frac{m_v}{m_v + (1 - m_v)\rho_s} \tag{5}$$

where ρ_s is the bulk density of the solid material. According to [1], a typical value of ρ_s for leaves is 0.3 g/cm^3. The range of m_g extends from 0 to about 0.9, and the corresponding range of m_v is 0 to 0.7 (for $\rho_s \approx 0.3$).

Then, we can use the dielectric model introduced in section 4-9.2 of [1] to compute the real and imaginary part of relative permittivity of vegetation material.

2.2 Permittivity of canopy constituents

Accordingly, Ulaby and ElRayes [5] introduced a linear model for the permittivity of vegetation in the form of an additive mixture of three components:

$$\varepsilon_v = \varepsilon_r + v_{fw}\varepsilon_w + v_{bw}\varepsilon_b \tag{6}$$

where ε_r is a nondispersive residual component to be determined empirically, ε_w and ε_b are the complex permittivities of free water and bound water, respectively, and v_{fw} and v_{bw} are their associated volume fractions. The real and imaginary parts of ε_v are

$$\varepsilon'_v = \varepsilon'_r + v_{fw}\varepsilon'_w + v_{bw}\varepsilon'_b \tag{7}$$

$$\varepsilon''_v = v_{fw}\varepsilon''_w + v_{bw}\varepsilon''_b \tag{8}$$

(1) Free water in leaves

The free water in vegetation includes low concentrations of salts and sugars (salinity S seldom exceeds 15 psu), the expression for ε''_w requires the addition of a conductivity term. That is,

$$\varepsilon'_w = \varepsilon_{w\infty} + \frac{\varepsilon_{w0} - \varepsilon_{w\infty}}{1 + (f/f_0)^2} \tag{9}$$

$$\varepsilon_w'' = \frac{(f/f_0)(\varepsilon_{w0} - \varepsilon_{w\infty})}{1 + (f/f_0)^2} + \frac{\sigma_i}{2\pi\varepsilon_0 f} \tag{10}$$

where f_0 (GHz) is the relaxation frequency of free water, f (GHz) is the frequency of the signal. The ionic conductivity σ_i (g/kg) is a function of the water salinity S and the temperature T ($^\circ C$) [6]

$$\sigma(T, S) = \sigma(T, 35) \cdot P(S) \cdot Q(T, S) \tag{11}$$

$$\sigma(T, 35) = 2.903602 + 8.607 \cdot 10^{-2}T + 4.738817 \cdot 10^{-4}T^2 - 2.991 \cdot 10^{-6}T^3 + 4.3041 \cdot 10^{-9}T^4 \tag{12}$$

$$P(S) = S\frac{37.5109 + 5.45216S + 0.014409S^2}{1004.75 + 182.283S + S^2} \tag{13}$$

$$Q(T, S) = 1 + \frac{\alpha_0(T - 15)}{T + \alpha_1} \tag{14}$$

$$\alpha_0 = \frac{6.9431 + 3.2841S - 0.099486S^2}{84.85 + 69.024S + S^2} \tag{15}$$

$$\alpha_1 = 49.843 - 0.2276S + 0.00198S^2 \tag{16}$$

According to Section 4-2 and Section 4-9 in [1], at $T = 22^\circ C$, the relaxation frequency of water is 18 GHz, and the expressions for ε_w' and ε_w'' become [6]

$$\varepsilon_w' = 4.9 + \frac{74.4}{1 + (f/18)^2} \tag{17}$$

$$\varepsilon_w'' = \frac{74.4(f/18)}{1 + (f/18)^2} + \frac{18\sigma_i}{f} \tag{18}$$

$$\sigma_i \approx 0.17S - 0.0013S^2 \tag{19}$$

where S = 15 g/kg is used in the following experiments.

(2) Bound water in leaves

According the dielectric measurements for sucrose-water mixtures [5]

$$\varepsilon_b' = 2.9 + \frac{55(1 + \sqrt{f/0.36})}{(1 + \sqrt{f/0.36})^2 + (f/0.36)} \tag{20}$$

$$\varepsilon_b'' = \frac{55\sqrt{f/0.36}}{(1 + \sqrt{f/0.36})^2 + (f/0.36)} \tag{21}$$

(3) Empirical fits

By fitting the measured dielectric data to the dielectric model, the remaining quantities in Eq.(7) and Eq.(8) were found to assume the forms

$$\varepsilon_r = 1.7 - 0.74m_g + 6.16m_g^2 \tag{22}$$

$$v_{fw} = m_g(0.55m_g - 0.076) \tag{23}$$

$$v_{bw} = \frac{4.64m_g^2}{1 + 7.36m_g^2} \tag{24}$$

2.3 Extinction and scattering in a Rayleigh medium

Since the small leaves and needles of winter wheat can be treated smaller than the incident C band wave, winter wheat canopies are modelled as an equivalent spherical Rayleigh scatterers with the same size and mass. The scattering coefficient of Rayleigh particle is computed as

$$\begin{aligned} k_s &= \frac{8\pi}{3} N_v k^4 r^6 |K|^2 \\ &= 2v k^4 r^3 |K|^2 \end{aligned} \tag{25}$$

$$v = \left(\frac{4}{3}\pi r^3\right) N_v \tag{26}$$

$$u_l(z) = N_v(z) A_l \tag{27}$$

$$L = \int_{z=0}^{z=H} u_l(z) dz \tag{28}$$

and K is defined by

$$K = \frac{n^2 - 1}{n^2 + 2} = \frac{\varepsilon_v - 1}{\varepsilon_v + 2} \tag{29}$$

where $k = 2\pi/\lambda_b$ is the wavenumber in air, r (m) is the sphere of radius, v is the volume fraction of scatterers, N_v is the number of particles per m^3, u_l (m^2) is one-sided leaf area per m^3, H (m) is the thickness of the Rayleigh medium, $\varepsilon_v = n^2 = \varepsilon_p/\varepsilon_b$ is the permittivity of the sphere material, ε_p is the permittivity of the sphere material. When the background medium is air, as is true in the atmosphere, we have $\varepsilon_b = 1$.

The absorption coefficient is computed as

$$k_a = v k \varepsilon_v'' \left| \frac{3}{\varepsilon_v + 2} \right|^2 \tag{30}$$

Then, we can get the extinction coefficient

$$k_e = k_s + k_a \tag{31}$$

During the following experiments, we will set the volume fraction v of wheat scatterers equal 0.005 [7]. The wheat particle radius equal $0.01m$.

3 Bottom surface backscattering coefficient

3.1 Permittivity of soils

Similar as Section 2.2, Dobson et al. [8] developed the following semiempirical model for permittivity of soils ε_s

$$\varepsilon_s' = [1 + 0.66\rho_b + m_{v_s}^{\beta_1} (\varepsilon_w')^{\alpha} - m_v]^{1/\alpha} \tag{32}$$

$$\varepsilon_s'' = m_{v_s}^{\beta_2} \varepsilon_w'' \tag{33}$$

where ρ_b is the bulk density of the soil in g/cm^3 (if the value of ρ_b is unknown, it is recommended that the typical value of 1.7 g/cm^3 be used), m_{v_s} is the volumetric moisture content in g/cm^3, and ε_w is the permittivity of water.

$$m_{v_s} = \frac{V_w}{V_{\text{dry}}} = \frac{W_w \rho_b}{W_{\text{dry}} \rho_w} \qquad (g/cm^3) \tag{34}$$

where V_w is the water volume, V_{dry} is volume of the dry sample, W_w and W_{dry} are the weights of the water in the sample and of the dry sample, respectively; $\rho_w = 1 g/cm^3$ is the density of water.

$$\varepsilon'_w = \varepsilon_{w\infty} + \frac{\varepsilon_{w0} - \varepsilon_{w\infty}}{1 + (2\pi f \tau_w)^2} \tag{35}$$

$$\varepsilon''_w = \frac{2\pi f \tau_w (\varepsilon_{w0} - \varepsilon_{w\infty})}{1 + (2\pi f \tau_w)^2} + \left(\frac{2.65 - \rho_b}{2.65 m_{v_s}}\right) \frac{\sigma}{2\pi \varepsilon_0 f} \tag{36}$$

where $\varepsilon_0 = 8.85410^{-12} F/m$. The exponents α, β_1, β_2 and the effective conductivity σ are related to the soil properties. Their empirically determined expressions are:

$$\alpha = 0.65 \tag{37}$$

$$\beta_1 = 1.27 - 0.519S - 0.152C \tag{38}$$

$$\beta_2 = 2.06 - 0.928S - 0.255C \tag{39}$$

$$\sigma = -1.645 + 1.939\rho_b - 2.256S + 1.594C \tag{40}$$

The empirical computation of other parameters are given by

$$\varepsilon_{w\infty} = 4.9 \tag{41}$$

$$2\pi\tau_w(T) = 1.1109 \times 10^{-10} - 3.842 \times 10^{-12} T + 6.938 \times 10^{-14} T^2 - 5.096 \times 10^{-16} T^3 \tag{42}$$

$$f_0 = (2\pi\tau_w)^{-1} \tag{43}$$

$$\varepsilon_{w0}(T) = 88.045 - 0.4147T + 6.295 \times 10^{-4} T^2 + 1.075 \times 10^{-5} T^3 \tag{44}$$

During the following experiments, the land surface temperature is acquired using MOD11A1 V6 product.

3.2 Backscattering coefficient estimation

The initial backscattering values are computed with an empirical method provided by [9].

$$p = \frac{\sigma^0_{hh}}{\sigma^0_{vv}} = \left[1 - \left(\frac{2\theta}{\pi}\right)^{\alpha} e^{-kd}\right]^2 \tag{45}$$

where θ is the incidence angle in radians, $k = 2\pi/\lambda$, d (m) is the rms height, and

$$\alpha = \frac{1}{3\Gamma_0} \tag{46}$$

with Γ_0 representing the surface (Fresnel) reflectivity at normal incidence,

$$\Gamma_0 = \left|\frac{1 - \sqrt{\varepsilon_s}}{1 + \sqrt{\varepsilon_s}}\right|^2 \tag{47}$$

where ε_s is the permittivity of soil.

Then, the backscattering coefficient of the bottom surface in the absence of the crop layer is

$$\sigma^0_{s_{vv}} = 0.7\left[1 - e^{-0.65(kd)^{1.8}}\right] \frac{cos^3\theta}{\sqrt{p}} [\Gamma_v(\theta) + \Gamma_h(\theta)] \tag{48}$$

For a plane wave incident upon a planar boundary from medium 1 to medium 2, $\Gamma_v(\theta)$ and $\Gamma_h(\theta)$ are computed according to the Fresnel reflection and transmission coefficients and associated reflectivities and transmissivities.

When the soil is covered by winter wheat, the bacscattering from soil will be seriously reduced because of the two-way transmissivity of the vegetation.

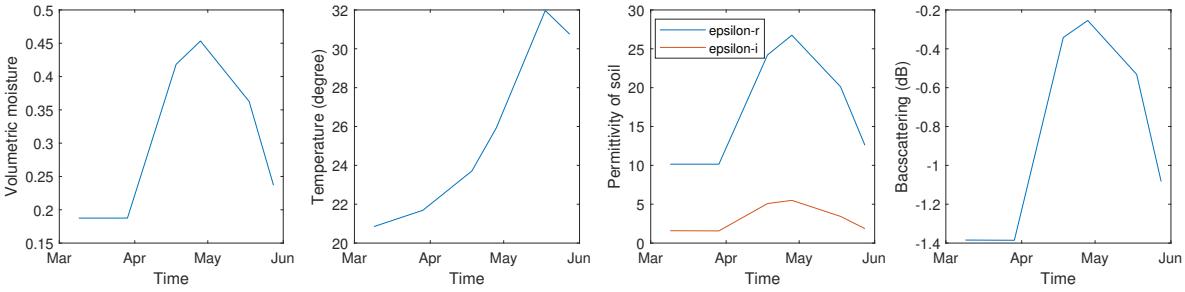

Figure 1: Bare soil bacscattering $\sigma^0_{s_{vv}}$ estimation using in-situ soil moisture data acquired over North China Plain, with $\theta = 39.5925^o$, $d = 0.025$, frequency $f = 5.405(\text{GHz})$, $\rho_b = 1.7g/cm^3$. The used land surface temperature is acquired using MOD11A1 V6 product. For the local soil, we assume that sand account for 25%, silt account for 50% and clay account for 25%.

4 Radiative transfer method

The radiative-transfer approach deals with the transport of energy through a medium containing particles and assumes that there is no correlation between the fields scattered by different particles. This assumption allows the incoherent addition of the powers associated with multiple scattering contributions, rather than the addition of their electric fields.

Most terrestrial media are not composed of spherical particles, which means that scattering by the particles is, in general, wave-polarization dependent. Also, the scattering medium is bounded by a lower surface (ground) and sometimes by an upper surface. Reflection by and transmission across surface boundaries also are polarization dependent. The vector radiative transfer equation can be expressed as

$$\frac{d\mathbf{I}(\mathbf{R},\hat{\mathbf{s}})}{ds} = -\mathbf{k}_e\mathbf{I}(\mathbf{R},\hat{\mathbf{s}}) - k_{a,b}\mathbf{I}(\mathbf{R},\hat{\mathbf{s}}) + \iint_{4\pi} \Psi(\hat{\mathbf{s}},\hat{\mathbf{s}}')\mathbf{I}(\mathbf{R},\hat{\mathbf{s}})d\Omega' \tag{49}$$

where $\mathbf{k}_e$ is the extinction matrix, $\mathbf{I}$ is a 4×1 vector representing the vector specific intensity of a plane wave with electric field, $\hat{\mathbf{s}}$ is the propagation direction and $\mathbf{R}$ is a vector from the center of the coordinate system to the location of the differential volume under consideration and Ψ phase matrix.

Here, we use iterative-solution technique to solve the radiative transfer equation. The procedure starts by computing the zero-order solution, which ignores scattering, except for its contribution to extinction. The zero-order solution then serves as a source function for computing the first-order solution. Taking the vv channel for example, with iterative-solution method, we can get the backscattering coefficients for vv with total backscattering transformation matrix $\mathcal{T}_t(\mu_i, \phi_i + \pi; -\mu_i, \phi_i)$

$$\sigma^o_{vv}(\theta_i) = \gamma^2\sigma^o_{s_{vv}}(\theta_i) + 4\pi cos\theta_i[\mathcal{T}_t]_{11} \tag{50}$$

where γ^2 is the two-way transmissivity of the middle layer, $[\mathcal{T}_t]_{11}$ is the backscattering transformation matrix for vv polarization.

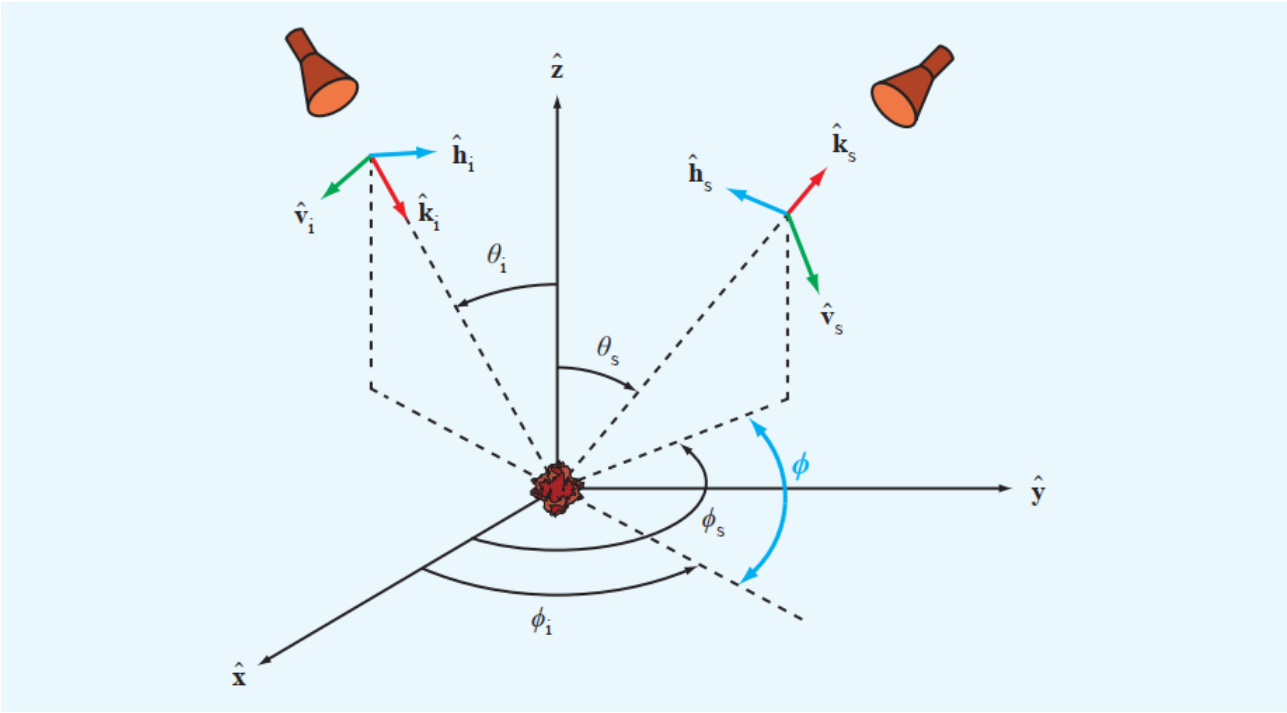

Figure 2: Incident and scattering directions for a point scatterer. Phase matrix of a random medium containing spherical Rayleigh scatterers with incidence along (θ_i,ϕ_i) and scattering along (θ_s,ϕ_s)

If small leaves and needles in vegetation canopies are not spherical in shape but small in size relative to λ, it may be modeled as an equivalent sphere with the same size and mass as the actual leaves and needles. The canopy scattering can be computed using the Rayleigh approximation. In the plane of incidence ($\phi_s = \phi_i$), all nondiagonal terms are zero, and the diagonal terms simplify to

$$\begin{aligned}\psi_{11} &= \frac{3k_s}{8\pi}[\sin^2\theta_s\sin^2\theta_i + \cos^2\theta_s\cos^2\theta_i\cos^2(\phi_s-\phi_i) + 2\sin\theta_s\sin\theta_i\cos\theta_s\cos\theta_i\cos(\phi_s-\phi_i)] \\ &= \frac{3k_s}{8\pi}(\sin\theta_s\sin\theta_i + \cos\theta_s\cos\theta_i)^2\end{aligned} \tag{51}$$

Moreover, if $\theta_s = \theta_i$ (in addition to ($\phi_s = \phi_i$)),

$$\psi_{11} = \frac{3k_s}{8\pi} \tag{52}$$

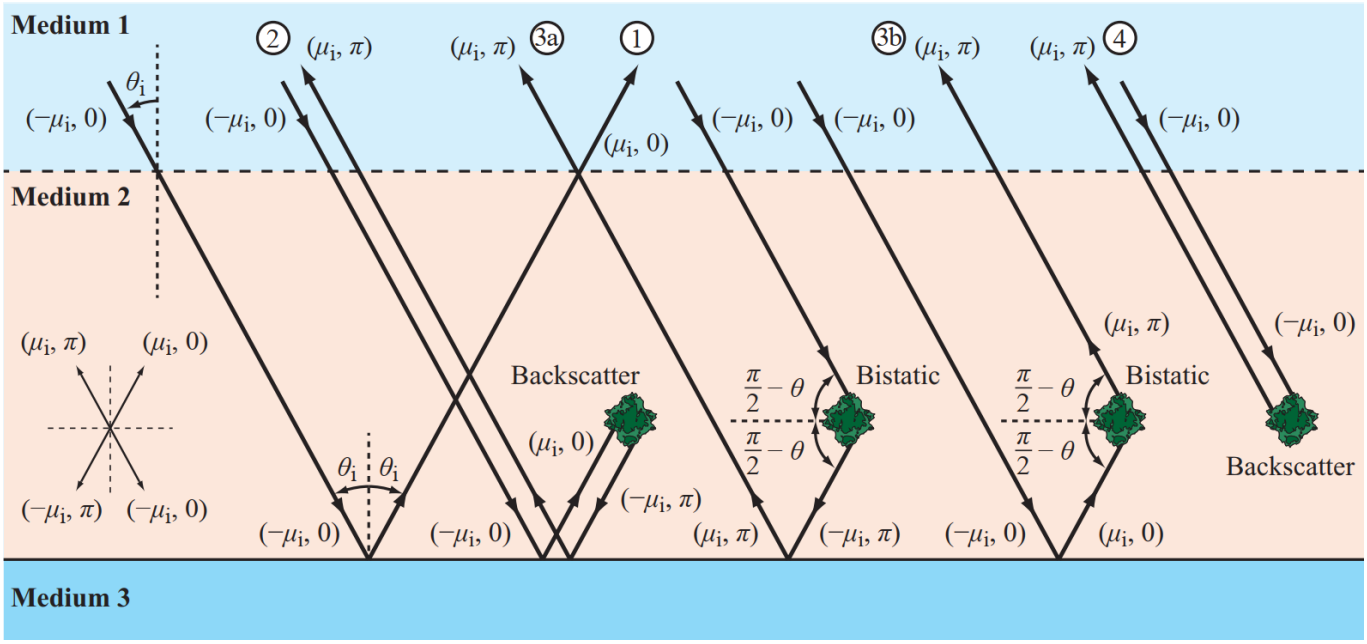

Figure 3: Volume scattering mechanisms.

With the first-order solution of the radial transfer equation, we get

$$\begin{aligned}\mathbf{I}_1^+(\theta_i,\phi_i,0) = {} & \gamma^2\mathbf{R}(\theta_i)\mathbf{I}_0^i\sigma(\phi_s-\phi_i=\pi) \\ & + \Big[\gamma^2\mathbf{R}(\theta_i)\Psi(-\mu_i,\phi_i+\pi;\mu_i,\phi_i)\mathbf{R}(\theta_i)\frac{\mu_i}{2k_e}(1-\gamma^2) \\ & + H\gamma^2\Psi(-\mu_i,\phi_i+\pi;-\mu_i,\phi_i)\mathbf{R}(\theta_i) \\ & + H\gamma^2\mathbf{R}(\theta_i)\Psi(\mu_i,\phi_i+\pi;\mu_i,\phi_i) \\ & + \Psi(\mu_i,\phi_i+\pi;-\mu_i,\phi_i)\frac{\mu_i}{2k_e}(1-\gamma^2)\Big]\frac{\mathbf{I}_0^i}{\mu_i}\end{aligned} \tag{53}$$

where $\mathbf{I}_0^i$ is the zeroth-order solution, $\mathbf{R}$ is the reflectivity matrices. The five terms of Eq. (53) are diagrammed in Fig. 3. The first term does not contribute to the backscatter, except at normal incidence. After deletion of the first term in Eq. (53) and comparison with Eq. (50), we obtain the transformation matrix

$$\begin{aligned}\mathcal{T}_t(\mu_i,\phi_i+\pi;-\mu_i,\phi_i) = {} & \frac{1-\gamma^2}{2k_e}[\Psi(\mu_i,\phi_i+\pi;-\mu_i,\phi_i) \\ & + \gamma^2\mathbf{R}(\theta_i)\Psi(-\mu_i,\phi_i+\pi;\mu_i,\phi_i)\mathbf{R}(\theta_i)] \\ & + \frac{H\gamma^2}{cos\theta_i}[\Psi(-\mu_i,\phi_i+\pi;-\mu_i,\phi_i)\mathbf{R}(\theta_i) \\ & + \mathbf{R}(\theta_i)\Psi(\mu_i,\phi_i+\pi;\mu_i,\phi_i)]\end{aligned} \tag{54}$$

If the middle layer is composed of Rayleigh particles and our interest is in vv polarization, we use Eq.(50), which corresponds to Eq.(54) after replacing $\mathbf{R}$ with Γ_v and Ψ with ψ_{11}. Hence,

$$
\begin{aligned}
\sigma^o_{vv}(\theta_i) =& \gamma^2\sigma^o_{s_{vv}}(\theta_i) + 4\pi cos\theta_i[\mathcal{T}_t]_{11} \\
=& \gamma^2\sigma^o_{s_{vv}}(\theta_i) + 4\pi cos\theta_i \frac{1-\gamma^2}{2k_e}\frac{3k_s}{8\pi} \\
&+ 4\pi cos\theta_i\gamma^2\Gamma^2\frac{1-\gamma^2}{2k_e}\frac{3k_s}{8\pi} \\
&+ 4\pi cos\theta_i\frac{H\gamma^2}{cos\theta_i}\left(2\Gamma^2\frac{3k_s}{8\pi}\right) \\
=& \gamma^2\sigma^o_{s_{vv}}(\theta_i) + \frac{3}{4}acos\theta_i(1-\gamma^2)(1+\Gamma^2\gamma^2) + 3k_sH\Gamma\gamma^2
\end{aligned}
\tag{55}
$$

where $\Gamma = \Gamma_v$, $a = k_s/k_e$ is the single-scattering albedo, H is the height of the medium 2 in Fig.3. We refer to this expression as the single-scattering radiative transfer model with Rayleigh scatterers (SSRT) under the incoherent addition assumption.

The radiative transfer model adds all energy sources incoherently, without regard to phase interference. The last term in Eq. (55) represents the incoherent addition of terms "3a" and "3b" in Fig. 3, which (for hh and vv polarizations) undergo the same phase delays due to propagation, the same phase changes due to specular reflection by the underlying ground surface, and probably the same phase changes introduced by bistatic scattering by the same differential volume. Hence, the two contributions should be in phase, in which case the magnitude of the last term in Eq. (55) should be increased by a factor of 2. Consequently

$$
\sigma^o_{vv}(\theta_i) = \gamma^2\sigma^o_{s_{vv}}(\theta_i) + \frac{3}{4}acos\theta_i(1-\gamma^2)(1+\Gamma^2\gamma^2) + 6k_sH\Gamma\gamma^2 \tag{56}
$$

$$
\gamma = e^{-\tau} \tag{57}
$$

$$
\tau = k_eH\mathrm{sec}\theta_i \tag{58}
$$

And the backscatters contributed by the canopy is

$$
\begin{aligned}
\sigma^o_{c_{vv}}(\theta_i) &= 4\pi cos\theta_i\frac{1-\gamma^2}{2k_e}\Psi(\mu_i, \phi_i+\pi; -\mu_i, \phi_i) \\
&= 4\pi cos\theta_i\frac{1-\gamma^2}{2k_e}\frac{3k_s}{8\pi} \\
&= \frac{3a}{4}cos\theta_i(1-\gamma^2)
\end{aligned}
\tag{59}
$$

Then, we can transfer it to dB value using $\sigma^0_{vv}(\mathrm{dB}) = 10\times\log_{10}(\sigma^0_{vv})$.

5 Experimental results and discussion

In this section, we will test the model with some Sentinel-2 generated data acquired over North China Plain. The two test areas are different for the acquisition incidence angle, the length of time series. Empirical extinction coefficient are used, with $k_e = 1.695$, $a = 0.015$. The scattering and absorption coefficient k_s and k_a are estimated according to Section 2.3.

5.1 Test winter wheat area 1

5.1.1 With empirical k_e and a

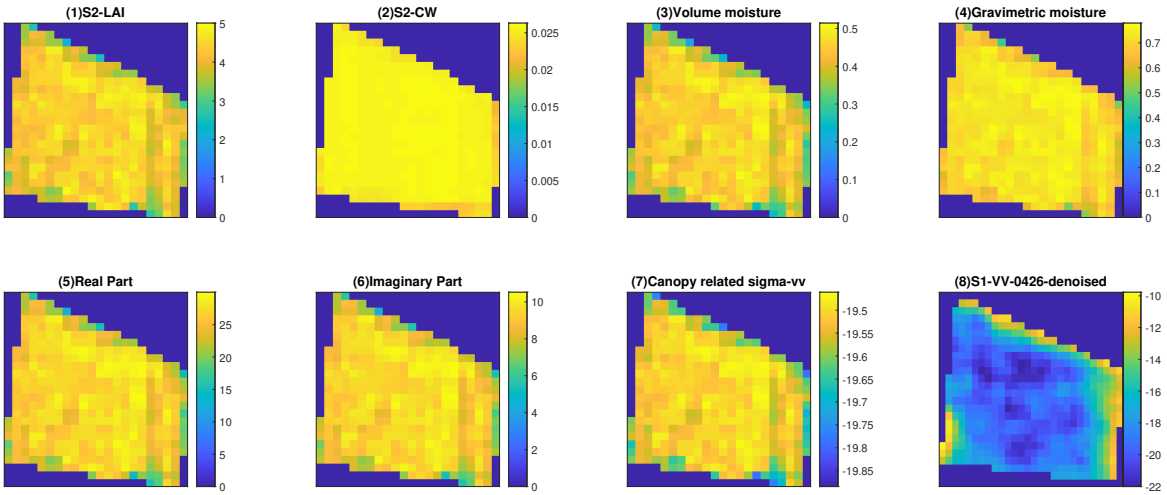

Figure 4: Backscattering value estimation with Sentinel-2 LAI, CW, vegetation height (0.7m), Sentinel-1 frequency (5.405 GHz), incidence angle (34.81^o), rms height (0.025m), single-scattering albedo (0.015) and extinction coefficient (1.695 Np/m). The boundary area values in Sentinel-1 VV image are very high due to the spatial coherence effect. The farmland are surrounded by big trees.

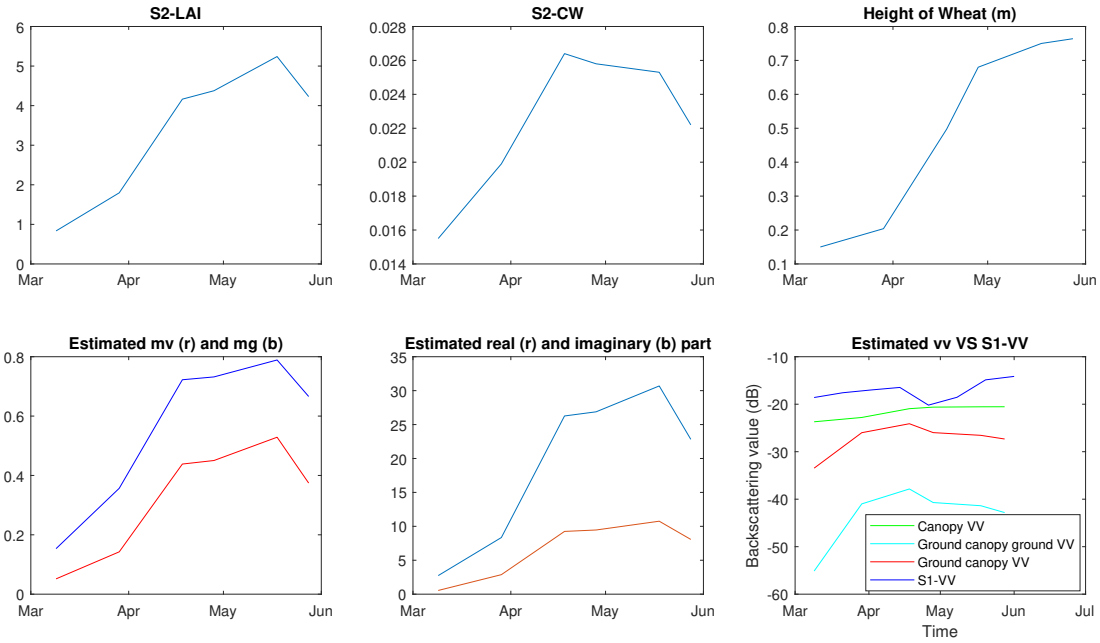

Figure 5: Time series backscattering value estimation. Normally, the VV backscattering values should increase during the growing of wheat. HS01 time series in Hengshui area, North China Plain is used.

5.1.2 With estimated k_s and k_a

The volume fraction $v = 0.005$ of wheat scatterers, the particle radius $r = 0.01m$ are used. Time series k_s and k_a are estimated according to Section 2.3.

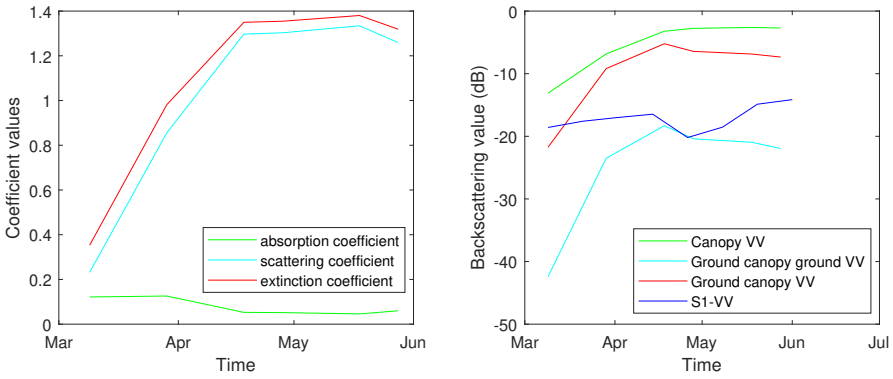

Figure 6: Time series backscattering value estimation.

5.2 Test winter wheat area 2

5.2.1 With empirical k_e and a

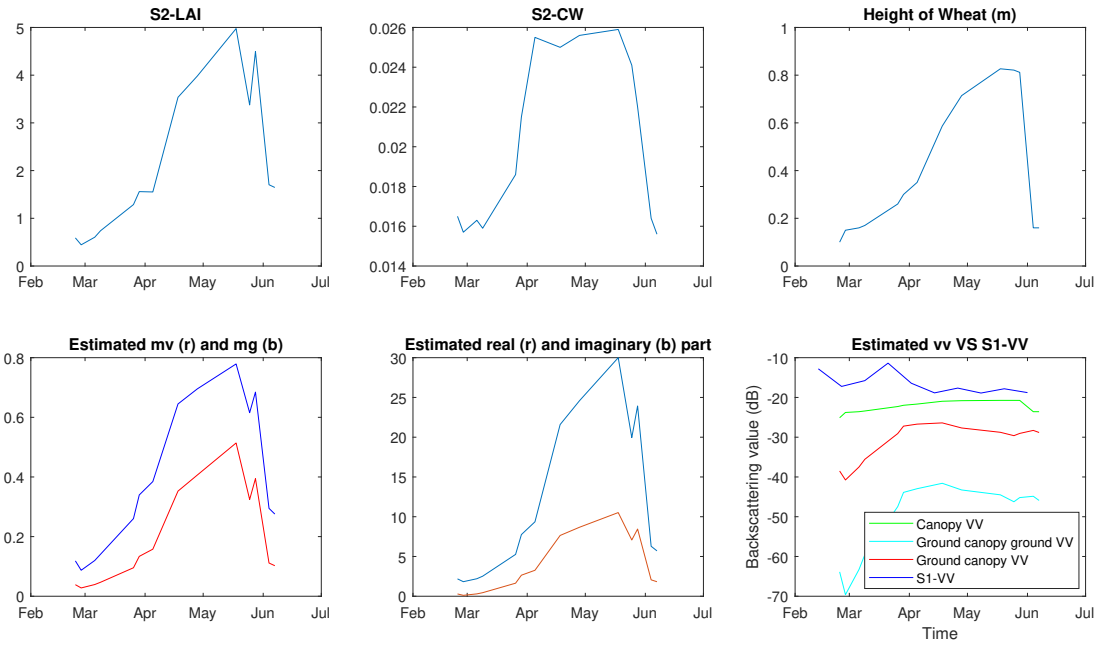

Figure 7: Time series backscattering value estimation. FC01 time series in Hengshui area, North China Plain is used. Backscattering value estimation with Sentinel-2 LAI, CW, Sentinel-1 frequency (5.405 GHz), incidence angle (39.593^o), rms height (0.025m), single-scattering albedo (0.015) and extinction coefficient (1.695 Np/m).

5.2.2 With estimated k_s and k_a

The used model parameters are the same as Section 5.1.2.

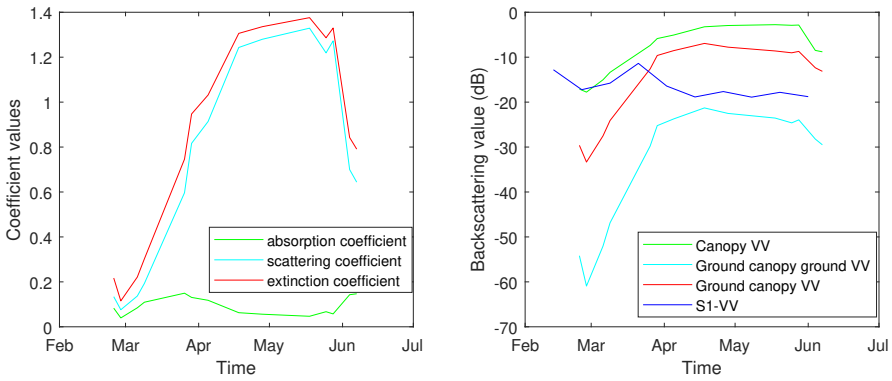

Figure 8: Time series backscattering value estimation.

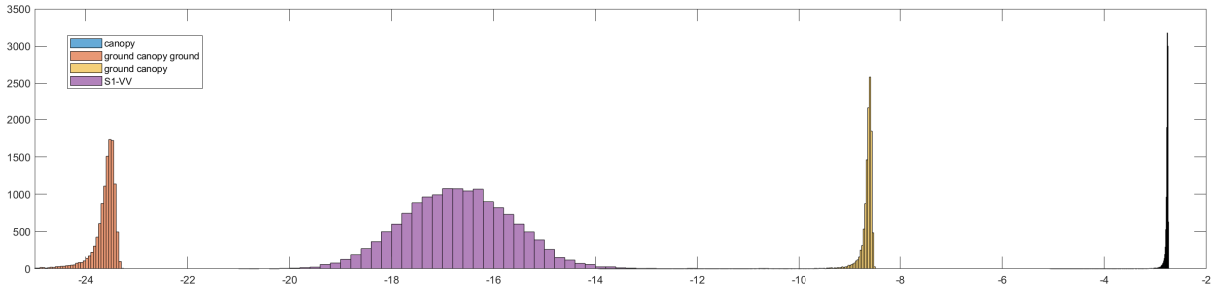

Figure 9: Comparison of different backscattering values. Multiple fields are used during the estimation.

It seems that the estimated backscattering values are too large when using estimated k_s and k_a. A constant may be needed to adjust the value.

6 Conclusion

In this report, only the VV backscattering related to canopies are analyzed. According to the experiments, a refined constant can be used to improve the results when using estimated scattering and absorption coefficient values. $T = 22°C$ is used when computing k_s and k_a. The permittivities of vegetation and soil are temperature depended, they need to be recalculated when dealing with long time series data.

References

[1] F. Ulaby and D. Long. *Microwave radar and radiometric remote sensing*. Artech House, 2015.

[2] C. Zhang, E. Pattey, J. Liu, H. Cai, J. Shang, and T. Dong. Retrieving leaf and canopy water content of winter wheat using vegetation water indices. *IEEE Journal of Selected Topics in Applied Earth Observations and Remote Sensing*, 11(1):112–126, 2017.

[3] A. Toure, K.P. Thomson, G. Edwards, R.J. Brown, and B.G. Brisco. Adaptation of the MIMICS backscattering model to the agricultural context-wheat and canola at L and C bands. *IEEE Transactions on Geoscience and Remote Sensing*, 32(1):47–61, 1994.

[4] C. Matzler. Microwave (1-100 Ghz) dielectric model of leaves. *IEEE Transactions on Geoscience and Remote Sensing*, 32(4):947–949, 1994.

[5] F.T. Ulaby, A. Tavakoli, and B.A. Thomas. Microwave propagation constant for a vegetation canopy with vertical stalks. *IEEE transactions on geoscience and remote sensing*, (6):714–725, 1987.

[6] C. ed. Mätzler. *Thermal microwave radiation: applications for remote sensing*, volume 52. Iet, 2006.

[7] T. Meyer, T. Jagdhuber, M. Piles, A. Fluhrer, and F. Jonard. Estimation of volume fraction and gravimetric moisture of winter wheat based on microwave attenuation: a field scale study. In *IGARSS 2019-2019 IEEE International Geoscience and Remote Sensing Symposium*, pages 5453–5456. IEEE, 2019.

[8] M.C. Dobson, F.T. Ulaby, M.T. Hallikainen, and M.A. El-Rayes. Microwave dielectric behavior of wet soil-part II: Dielectric mixing models. *IEEE Transactions on Geoscience and Remote Sensing*, (1):35–46, 1985.

[9] Y. Oh, K. Sarabandi, and F.T. Ulaby. An empirical model and an inversion technique for radar scattering from bare soil surfaces. *IEEE transactions on Geoscience and Remote Sensing*, 30(2):370–381, 1992.